

A New Strategy to Improve Coregistration of SPECT and MR Images in Patients with High Grade Glioma

Jean-Marc Tacchella^{1,2}, Elodie Roullot², Muriel Lefort¹, Mike-Ely Cohen¹, Rémy Guillevin^{1,3}, Grégorio Petrirena⁴, Jean-Yves Delattre⁴, Marie-Odile Habert^{1,5}, Nathanaëlle Yeni^{1,5}, Aurélie Kas^{1,5} and Frédérique Frouin¹

Abstract— This paper proposes a new strategy to optimize the coregistration of Technetium-99m Sestamibi SPECT and MRI data in case of patients with high grade glioma. It consists in a personalized approach which selects, for each data set, the best registration method among several ones. To achieve this selection, a quantitative dedicated evaluation criterion based on the average intensities within specific anatomical structures corresponding to physiological areas of uptake of Sestamibi was defined. The strategy was applied to sixty-two data sets using nine registration methods based on mutual information and chamfer distance registration approaches, with different settings. It was implemented within the Anatomist/Brainvisa environment, using its basic registration functions. The visual evaluation by experts indicated that this strategy provides 60% good quality registrations, and 26% intermediate quality ones. Compared to the single use of the best global registration method, the number of registrations of good quality was multiplied by 1.4 when using the data specific strategy.

I. INTRODUCTION

Glioma is the most frequent primary central nervous system tumor in adults. Despite progress in biological knowledge and therapy, the prognosis of patients with high-grade glioma remains poor. Structural and functional neuroimaging enables the non-invasive evaluation of glioma and has a crucial role in the management of these patients. Technetium-99m labeled Sestamibi (MIBI) is a radiopharmaceutical that accumulates in malignant gliomas. The usefulness of MIBI brain single-photon emission computed tomography (SPECT) has been shown in distinguishing treatment-related radionecrosis from tumor recurrence, and has been suggested in therapy management [1]. Ideally, this analysis should be performed after coregistration with high-contrast anatomical images (e.g., MRI) in order to combine the functional and morphological information. However, this registration procedure cannot be completed easily in clinical practice. Indeed, because of the

distribution of MIBI in intracranial structures (low uptake in normal parenchyma contrasting with high uptake in oculomotor muscles, choroid plexus and pituitary gland) the problem of matching MRI and SPECT data cannot be fully solved using a conventional registration method. Manual registration is an alternate solution, but this task is both tedious and labor-intensive (about 30 min). A conventional way to classify registration algorithms [2,3] is to distinguish the feature based algorithms which require the extraction of primitives (points, edges or surfaces) before the matching step, and the iconic based algorithms which use similarities in voxels intensities to register images. The Chamfer Distance (CD) [4] is a conventional similarity measure used in feature based algorithms whereas the Mutual Information (MI) [5] is often used in iconic based algorithms. Iconic based methods are often preferred over feature based similarity measures because it avoids the feature extraction step, which needs an additional tuning of parameters. The efficiency of the registration algorithms depends on different factors, such as the matching type (inter or intra patient data), the body part investigated, the imaging modalities, the specific uptake of the tracer for SPECT, and the settings of the registration algorithms including initialization, similarity criterion, optimization. Therefore, the customization of these algorithms can prove to be a difficult and time-consuming task. To help users in their choices, some studies have compared different registration methods [6,7,8]. For these tests, different algorithms were applied to the same database to determine the best algorithm over the entire database. But the globally best algorithm can fail to correctly register individual datasets among a database. That is why we propose a new registration strategy that consists in selecting, the best registration method among several ones for each dataset thanks to a dedicated quantitative criterion based on *a priori* knowledge. In our specific clinical application, the *a priori* is related to the physiological uptake of MIBI.

II. METHODS

The proposed SPECT to MRI registration strategy is based on three successive steps, as shown in Figure 1. For each dataset, nine registration methods (M_n , $1 \leq n \leq 9$) were first applied, each registration method was then evaluated using a quantitative criterion to select the best method (M^*). A visual reading was finally performed to indicate whether the registration proposed by M^* was correct or not.

J. Tacchella, M. Lefort, M. Cohen, R. Guillevin, M. Habert, N. Yeni, A. Kas and F. Frouin are with UPMC INSERM UMR_S 678, Laboratoire d'Imagerie Fonctionnelle, Paris, France. frouin@imed.jussieu.fr

J. Tacchella and E. Roullot are with ESME Sudria, Laboratoire PRIAM, Ivry sur Seine, France.

R. Guillevin is with Université de Poitiers and CHU Poitiers, Service de radiologie, Poitiers, France

G. Petrirena and J. Delattre are with AP-HP, CHU Pitié-Salpêtrière, Service de neuro-oncologie, Paris, France

MO. Habert, N. Yen and A. Kas are with AP-HP, CHU Pitié-Salpêtrière, Service de médecine nucléaire, Paris, France

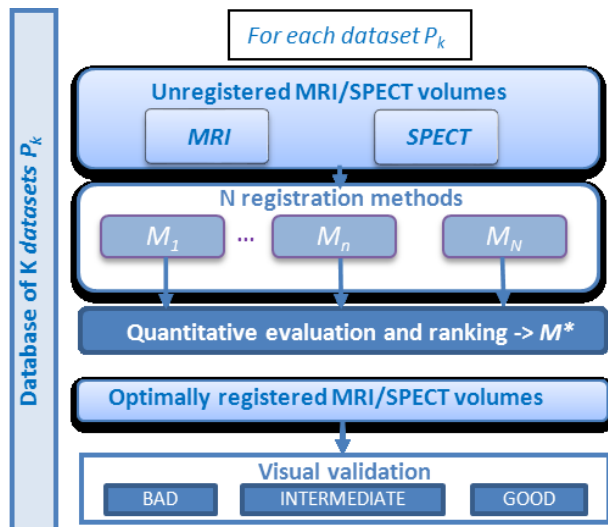


Figure 1. Flowchart of the registration strategy

A. Database

The database includes 62 datasets of patients presenting recurrent high grade glioma. Each dataset is composed of one T1-weighted MRI obtained after the injection of Gadolinium-DTPA (Signa Hdxt 3T, GE) and one MIBI SPECT volume acquired after injection of MIBI (Irix, Philips). The two exams were performed less than 72 hours apart. The SPECT volumes are composed of 66 axial slices of isotropic voxels (2.3 mm according to each direction). The MR volumes contain 248 axial slices with a thickness of 0.69 mm and a pixel size of 0.48x0.48 mm². For the registration, SPECT volumes before and after attenuation correction were considered

B. Registration methods

Since the registration concerned intra-patient data and the examined region was the brain, a rigid transformation (3 translations and 3 rotation angles) was chosen. Nine 3D rigid registration methods listed in Table 1 were implemented within the public user version of the Anatomist BrainVISA environment[9] (http://brainvisa.info/index_f.html). Different tunings of the “AimsMIRegister” function lead to three MI based methods whereas six CD based methods were similarly derived from the “VipMatching” function.

TABLE I. DEFINITION OF THE NINE REGISTRATION METHODS. SEE TEXT FOR THE DEFINITION OF ACRONYMS VISUAL ASSESSMENT OF AUTOMATICALLY DEFINED ROI

	Similarity Measure	Sub-sampling	MRI edge	SPECT edge	Transformation
M1	MI	MRI/8	None	none	i
M2	MI	SPECT	None	none	d
M3	MI	SPECT	None	None	i
M4	CD	SPECT	T-MO	T-AC	d
M5	CD	SPECT	T-MO	T-AC	i
M6	CD	SPECT	T-MO	D-A	d
M7	CD	SPECT	T-MO	D-A	i
M8	CD	SPECT	T-MO	D-AC	d
M9	CD	SPECT	T-MO	D-AC	i

a) Subsampling

For MI based methods, a step of sub-sampling was performed on the MRI image using a trilinear interpolation. For M1, the MRI dimension was divided by 8 (2 in each direction). For M2 and M3 the MRI image was subsampled to the resolution of the SPECT image with a volume reduction factor of about 80. Oversampling of SPECT data was not considered in that study.

b) Skull edge extraction

As the Chamfer Distance (CD) estimates a distance between contours in images, the CD based registration methods (M4 to M9) required the extraction of the skull edge from both MRI and SPECT images. The extraction of the binary mask of the head from the MRI image was based on a thresholding (T) to remove the image background and was completed by a set of morphological operations (MO) to fill and smooth the mask. A morphological gradient then provided the skull edge which was finally sub-sampled to the SPECT resolution using a nearest neighbor interpolation. The skull edge was extracted from the SPECT image according to three different ways: 1) by applying a threshold to the SPECT image after attenuation correction (T-AC), for M4 and M5; 2) by applying a Deriche filter [10] to the SPECT image after attenuation correction (D-AC), for M8 and M9; 3) by applying a Deriche filter to the SPECT image before attenuation correction (D-A), for M6 and M7. The external edges were then extracted from the images resulting from the Deriche filter to get the skull edge.

c) Transformation

The best “SPECT to MRI” transformation matrix could be estimated directly (d) by aligning the SPECT image on the MR image or indirectly (i) by aligning the MR image on the SPECT image, from which a “SPECT to MRI” transformation was obtained by matrix inversion. Finally this transformation matrix was applied to the SPECT image after attenuation correction, using a trilinear interpolation.

d) Optimization and initial values

The translation parameters of the transformation matrix were initialized from the center of gravity of the images and the rotation angles were initialized with a 0 value for all methods. The Powell’s optimization algorithm was used systematically to find the extreme values of the cost functions.

C. Quantitative evaluation and ranking

As the registration performance of one given method varied from one dataset to another, we chose to classify these methods to select the best one for a given dataset. We did not retain the similarity measures used by the image registration methods, since they did not match the visual criteria used by specialists. Thus, we decided to translate these visual criteria into a new quantitative evaluation criterion. It was based on physiological low and high uptake of Sestamibi within particular anatomical structures, and did not depend on pathological structures.

a) Segmentation of anatomical areas

Observations made by experts rely on the uptake of the tracer within some specific anatomical structures, outside the tumor. As the MIBI uptake is high in the pituitary gland and in the oculomotor muscles and low in the eyeballs, the computation of the new criterion required the segmentation of these structures. Due to the low spatial resolution of the SPECT image, the segmentation was difficult, even quite impossible, on SPECT data. Thus these areas were segmented on the MR images, and reported on the registered SPECT images. The eyeballs were segmented automatically using a spherical Hough Transform inside a region of interest around them, while the pituitary gland and the oculomotor muscles were semi-automatically segmented slice by slice by two independent operators using a 2D level set algorithm implemented in the MIPAV software (<http://mipav.cit.nih.gov/>). The different segmented areas were labeled and stored in a mask. This mask was then subsampled to the SPECT resolution using the nearest neighbor interpolation.

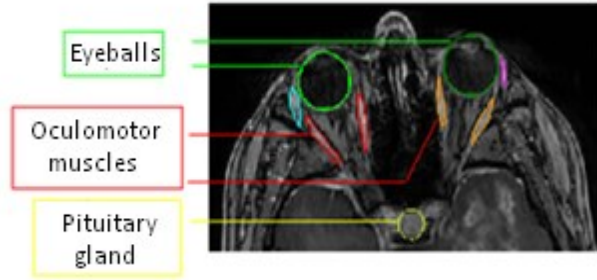


Figure 2. Segmentation of the eyeballs, the pituitary gland and the oculomotor muscles on MRI

b) Quantitative criterion

The definition of the quantitative criterion UC (Uptake Criterion) is based on the following assumption: registrations of good quality provide SPECT images that present high average intensities in the assumed high uptake areas and low average intensities in the assumed low uptake areas. Thus, for each registration method M_n , $UC(M_n)$ was computed as stated by (1):

$$UC(M_n) = \frac{1}{\text{Card}(V_{hu})} \sum_{p \in V_{hu}} I_{M_n}(p) - \frac{1}{\text{Card}(V_{lu})} \sum_{p \in V_{lu}} I_{M_n}(p), \quad (1)$$

$I_{M_n}(p)$ being the intensity of the registered SPECT image at voxel p , V_{hu} the volume corresponding to the high uptake regions, and V_{lu} the volume corresponding to the low uptake regions. The criterion $UC(M_n)$ was assumed to reach a maximum value for the best registered volume.

c) Ranking of the registration methods

For each dataset, the values of UC were computed for the nine registration methods, which allowed us to classify them. The method that was ranked first was considered as the best registration method for the considered dataset. However, the ranking did not ensure that the best method provided an

adequate registration. That is why a visual validation was necessary to check whether the SPECT image was correctly registered or not.

D. Visual validation

Visual validation by experts consisted in a qualitative assessment of the registration accuracy. The visual criteria used for this evaluation included the criteria mentioned above but also other hallmarks such as the high MIBI uptake in the choroid plexus, the nose and the skull. Each registration was scored according to three classes: good, intermediate, and bad.

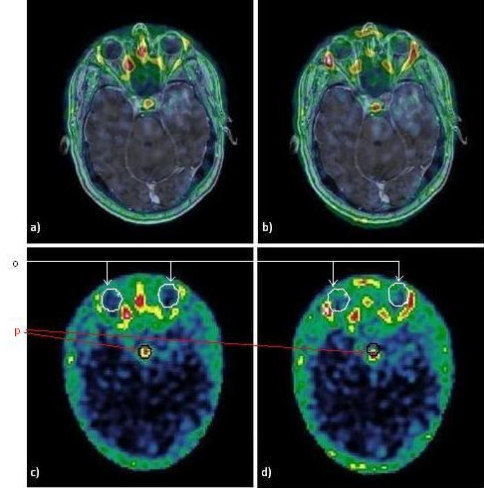


Figure 3. SPECT-MRI registrations performed on one specific dataset showing: a) a good registration using M^* (M_7 here) b) a bad registration (M_1 here). Superimposition of high uptake (in black) and low uptake (in white) areas on the SPECT images registered using c) M_7 and d) M_1 (p: pituitary gland, o: ocular globes)

III. RESULTS AND DISCUSSION

A. Relevance of the UC criterion

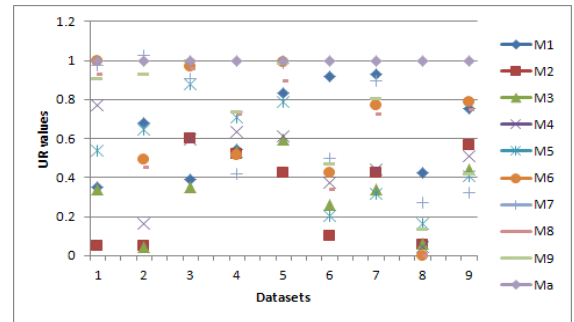


Figure 4. UR values computed for a subgroup of nine datasets using the segmentation of the first operator

To check the relevance of the UC criterion, manual registrations were performed by experts using the Anatomist software on a subgroup of nine datasets. These manual registrations (M_a) were considered as a “Gold Standard”. For each dataset, the ratio $UR = UC(M_n) / UC(M_a)$ was computed to compare the manual method with the automated ones. The UR values obtained for the nine datasets are displayed in Figure 4, $UC(M_n)$ values being computed using

the segmentation of the first operator. The manual registration method had the highest ratio for eight datasets out of nine. In the particular case of the second dataset, where the manual method obtained an UR value slightly lower than the best automatic method, M7, experts visually checked the results obtained by these two methods and considered that results were equivalent. Despite some minor inversions in the ranking of methods with very close UC values, results were quite similar when using the segmentation of the second operator. This result demonstrates the robustness of the UC criterion with respect to the segmentation. The fact that the “Gold Standard” method came first using the UC criterion proves its relevance to evaluate and classify the registration methods.

B. Performance of the strategy

On all 62 datasets, M1 came first in 33.9% of cases, M9 in 25.8%, M6 in 16.1%, M7 in 14%, M8 in 4.9%, M3 in 3.2%, M5 in 1.6%, M2 and M4 in 0% using the segmentation of the first operator. Using the segmentation of the second operator, these results only differed in 5 cases: in 3 cases, the first method was ranked second with the segmentation of the first operator, in the other 2 cases, third. For each dataset, the method ranking first with UC always gave better visual results than the other methods. However, these results could be very similar to the results obtained by other methods with a very close UC value and/or could be considered as not good enough by the physician. Thus the method M1 came first most of the time, but it was not the best method for the entire database. Indeed, applying the registration method M1 to the entire database provided 30% (19 datasets) of good quality registrations whereas the method M9 provided 40% (25 datasets) of good quality registrations. The method M9 was identified as the best global method for the 62 datasets. Among the 19 datasets correctly registered by M1, 12 are well registered and 7 are badly registered with M9. This clearly proves that the performance of methods varies from one dataset to another. As our strategy used the complementarity of methods, the results are globally improved, with 60% of good registration and 26% of intermediate quality registration.

C. Study limitation

The values of the criterion UC(Mn) depend on the anatomical structures that were manually segmented on MRI. Although the robustness of the UC criterion with respect to the segmentation was proven, the segmentation step is time consuming. Thus, future work will include the automation of this segmentation step.

Despite the data adapted proposed strategy, the proportion of intermediate registrations (26%) and bad registrations (14%) highlights the difficulty to register these studies using conventional metrics because of the specific uptake of the MIBI. In the present study we used 9 registration approaches based on two different criteria, which were directly available in the Anatomist/Brainvisa environment. This work was a first study to check the feasibility of this data adapted strategy and in order to improve the results, additional approaches such as the ones

used by SPM or FLIRT (FSL) will be further integrated in this environment. Some additional approaches such as hybrid methods [11, 12] coupling MI to feature information could be tested too.

Of course, the computation time depends on the number and type of registration methods used by the strategy. As an indication, CD based methods take a few seconds to register one MRI/SPECT dataset whereas MI based methods take about one minute. Thus, to save time, it is essential to keep only the “useful” methods, which can provide registrations of good quality. In the present study, the methods M2 to M5 could be removed.

IV. CONCLUSION

A new registration strategy was proposed which consisted in selecting among several methods based on either MI or CD optimization the most appropriate one for each dataset. To make this selection automatic, a new quantitative criterion based on the physiological behavior of the MIBI was defined. It was demonstrated on sixty-two datasets that this strategy provides better results than the conventional approaches which use only one registration method. Moreover, this strategy could be easily extended to other registration problems by adapting the quantitative evaluation criterion and choosing several adequate registration methods.

REFERENCES

- [1] F. Prigent-Le Jeune, et al, « Technetium-99m sestamibi brain SPECT in the follow-up of glioma for evaluation of response to chemotherapy: first results », *Eur J Nucl Med Mol Imaging*, vol. 31, n° 5, pp. 714-9, 2004.
- [2] B. Zitova and J. Flusser, « Image registration methods: a survey », *Image Vis. Comput.*, vol. 21, n° 11, pp. 977-1000, 2003.
- [3] J. B. Maintz and M. A. Viergever, « A survey of medical image registration. », *MedIA*, vol. 2, n° 1, pp. 1-36, 1998.
- [4] J.-F. Mangin, et al, «Fast Nonsupervised 3D Registration of PET and MR Images of the Brain». *J. Cereb. Blood Flow Metab.*, 14(5):749-762, Sep. 1994..
- [5] F. Maes, et al, « Multimodality image registration by maximization of mutual information », *IEEE Trans. Med. Imaging*, vol. 16, n° 2, pp. 187-198, 1997.
- [6] K. Murphy, et al, « Evaluation of Registration Methods on Thoracic CT: The EMPIRE10 Challenge », *IEEE Trans. Med. Imaging*, vol. 30, n° 11, pp. 1901-20, 2011.
- [7] A. Klein, et al, « Evaluation of 14 nonlinear deformation algorithms applied to human brain MRI registration », *NeuroImage*, vol. 46, n° 3, pp. 786-802, 2009.
- [8] A. Sarkar, et al, « Comparison of manual vs. automated multimodality (CT-MRI) image registration for brain tumors », *Medical Dosimetry*, vol. 30, n° 1, p. 20-4, 2005.
- [9] D. Rivière, et al., «BrainVISA : an extensible software environment for sharing multimodal neuroimaging data and processing tools.» In Proc. 15th HBM, 2009.
- [10] R. Deriche, « Using Canny’s criteria to derive a recursively implemented optimal edge detector », *International Journal of Computer Vision*, vol. 1, n° 2, pp. 167-87, 1987.
- [11] S. Bullich, et al, « Neurotransmission SPECT and MR registration combining mutual and gradient information », *Med Phys*, vol. 36, n° 11, pp. 4903-10, 2009.
- [12] J.-D. Lee, et al, « An automatic MRI/SPECT registration algorithm using image intensity and anatomical feature as matching characters: application on the evaluation of Parkinson’s disease », *Nuclear Medicine and Biology*, vol. 34, n° 4, p. 447-57, 2007.